Research Article | Vol. 14, No. 2 / 1 Feb 2023 / Biomedical Optics Express 550
Biomedical Optics EXPRESS

Evaluation of Slowfade Diamond as a buffer for STORM microscopy

HADJER BOUKHATEM,[1] BEATRICE DUREL,[2] MANON RAIMBAULT,[2] AUDREY LAURENT,[3,4] AND NICOLAS OLIVIER[1,*]

[1]*Laboratory for Optics and Biosciences (LOB), CNRS, INSERM, École polytechnique, Institut Polytechnique de Paris, 91120 Palaiseau, France*
[2]*Cell Imaging Platform, Structure Fédérative de Recherche Necker, INSERM US24, CNRS UMS3633, Paris, F-75015, France*
[3]*Université de Paris, Institut-Necker-Enfants-Malades, Inserm, CNRS, Paris, France*
[4]*École Doctorale BioSPC 562, Université de Paris, Paris, France*
[*]*nicolas.olivier@polytechnique.edu*

Abstract: We study the potential of the commercial mounting medium Slowfade diamond as a buffer for STORM microscopy. We show that although it does not work with the popular far-red dyes typically used for STORM imaging, such as Alexa Fluor 647, it performs really well with a wide variety of green-excited dyes such as Alexa Fluor 532, Alexa Fluor 555 or CF 568. Moreover, imaging can be performed several months after the samples are mounted in this environment and kept in the fridge, providing a convenient way to preserve samples for STORM imaging, as well as to keep calibration samples, for example for metrology or teaching in particular in imaging facilities.

1. Introduction

Single Molecule Localization Microscopy (SMLM) [1–5] is one of the most popular family of optical super-resolution methods since it requires a simple inverted microscope to achieve a gain in resolution of an order of magnitude and therefore enable the study of biological processes hidden behind the diffraction limit [6]. However, it requires samples to be prepared in a particular way, so as to enable stochastic switching between a fluorescent and a non-fluorescent state for the fluorophore imaged. In STORM microscopy this is achieved using standard dyes in a special chemical buffer that allows efficient transitions between a fluorescent an a nonfluorescent state [7–9]. Most STORM imaging is performed in a buffer fairly similar to the one used in the original demonstration [1,7], which combines a reducing thiol such as 2-Mercaptoethylamine/Cysteamine (MEA) or β-Mercaptoethanol (βME) and an enzymatic oxygen scavenging system based on the combination of glucose, glucose-oxydase and catalase. However, since this oxygen scavenging system acidifies with time [10,11], several alternatives have been proposed to alleviate this issue [12], including the use of other enzymatic systems such as PCA/PCD [13,14] and pyranose oxidase [14,15]. The blinking mechanism of dyes in this type of bufferis well studied [16–18] and several screens have been performed to identify the best fluorophores [19,20]. However, there have also been a few reports of different types of buffer aimed at simplifying the imaging protocols. In particular, Vectashield [21–23] and Prolong Diamond [24] are two commercial mounting media that have been found to work well for STORM imaging for different subsets of dye. Interestingly, while Vectashield worked best for the far-red dyes typically used in STORM such as Cy5 and Alexa Fluor 647, Prolong Diamond was reported to work best with Alexa Fluor 594 [24]. This ability to image red dyes motivated us in evaluating the properties of the related non-hardening mounting media Slowfade Diamond as a STORM buffer.

#473463 https://doi.org/10.1364/BOE.473463
Journal © 2023 Received 9 Sep 2022; revised 12 Dec 2022; accepted 20 Dec 2022; published 4 Jan 2023

Biomedical Optics EXPRESS

2. Methods

Optical setup and data acquisition

Dye Screening Dye screening was performed on an IX83 Inverted microscope (Olympus) using a 100x 1.3 NA objective (Olympus), and an Orca Fusion sCMOS camera (Hamamatsu). 3 free-space single mode lasers at 488 nm, 532 nm and 640 nm (Voltran, 100 mW, 40 mW and 100 mW) were used, as well as a 750 nm multimode laser (1.2 W Oxxius). The microscope was equipped with Chroma filters: 532 nm and 640 nm-excited fluorophores were imaged using a ZT532/640rpc 2-color dichroic mirror, and a ET605/70 or ET700-75 emission filter. Due to the double-deck design, where the top deck is equipped with only a dichroic mirror and the lower deck with full sets (Emission filter, dichroic mirror and excitation filter) the emitted light also goes through a T550lpxr dichroic (red fluorophores) or a T660lpxr dichroic (far-red fluorophores). 750 nm-excited fluorophores were imaged using a T760lpxr dichroic, and a ET810-90 emission filter. Similarly, the emitted light also goes through an additional T760lpxr dichroic. Green dyes excited at 488 nm were imaged using a GFP filter cube (49002 Chroma). For the dye screening 10,000-15,000 images were acquired with $\approx 40-60$ ms integration time using the slowest "ultra quiet scan" read-out speed of the camera and z-drift was corrected manually. The camera and microscope were controlled using micro-manager [25]. Laser power at 488 nm, 532 nm, 640 nm and 750 nm was typically between 1 and 4 kW.cm^{-2}.

Further imaging Further imaging of the best dyes identified was performed on a Nikon Ti:E microscope with an Apo TIRF 100X 1.49 Oil objective (Nikon) on an EMCCD camera (Quant EM:512SC, Photometrics), using the microscope's 1.5x extra magnification and resulting in a pixel size of 107 nm. The illumination came from a fiber-coupled laser combiner (L6CC Oxxius) equipped with a 640 nm 300 mW laser (LPX-640L-300-CSB-OE-900, Oxxius) and a 532 nm 500 mW laser (LPX-532L-500-CSB-OE-900, Oxxius). The filters used were a 4 band dichroic (Di03-R405/488/532/635-t1-25x36, Semrock) and the associated 4-band emission filter (FF01-446/510/581/703-25). This microscope was controlled using NIS, with camera exposure times of 30 ms and an EM gain of 1000. For most datasets, 20,000 frames were recorded.

Sample preparation and immunofluorescence staining

Dye Screening African green monkey kidney cells (COS-7) were cultured in DMEM-Glutamax (Gibco 10566016) supplemented with 10% FBS in a cell culture incubator (37°C and 5% CO_2). Cells were plated at low confluency on ethanol-cleaned 25 mm #1.5 thickness round coverglass (VWR) for imaging. Prior to fixation, all solutions were pre-warmed to 37∘C. 24h after plating, cells were pre-extracted for 30 s in 0.25% Triton X-100 (Sigma-Aldrich) in PHEM (60 mM PIPES, 25 mM HEPES, 10 mM EGTA, 4 mM MgSO4) washed in PHEM, fixed for 8 min in −20∘C Methanol (Sigma-Aldrich), then washed 3 times with PBS. The samples were then blocked for 1 hour in 5% BSA, before being incubated for 1.5 hour at room temperature with 1:500 Mouse anti alpha-tubulin (Sigma T6199) in 1% BSA diluted in PBS-0.2% Triton (BSA-PBST), followed by 3 washes in PBST, and then incubated for 1 hour in BSA-PBST with a secondary antibodies (see list in Table S1) and finally washed 3 times in PBST.

The sample were imaged in an Attofluor imaging chamber (Invitrogen, A7816), with 30 μl of Slowfade Diamond (Invitrogen S36963) and another 18 mm round coverglass on top to limit air exchanges.

Further imaging Human hCMEC/D3, hDBEC, and HDFa cells were cultured as in [26,27]. Briefly, Human hCMEC/D3 cells were grown in EBM-2 medium (Lonza) supplemented with 5% fetal calf serum 1.4 μM hydrocortisone (Lonza), 5 μg/mL ascorbic acid (Lonza), and 1 ng/mL b-FGF (Lonza) and grown on rat tail collagen-1 (BD Biosciences) coated flasks while hDBEC cells grown on rat tail collagen-1 (BD Biosciences) coated flasks in Endothelial Cell Growth Medium MV2 (Promocell) supplemented with Endothelial Cell Growth Medium Supplement Mix

Biomedical Optics EXPRESS

(Promocell). Cells were plated at low confluency on ethanol-cleaned 22x22mm #1.5 thickness square coverglass also coated with rat tail collagen-1. 24 hours after plating, the cells were rinsed in PHEM, then fixed in 4% PFA + Glutaraldehyde 0,2% in PHEM with 0,5% Triton for 12 min, then rinsed once in PBS 0.1% Triton and 3 times in PBS. The samples were then blocked for 1 hour in 3% BSA (Sigma-Aldrich A4503) at room temperature under gentle agitation, before being incubated for 1 hour at 37°C with 1:500 mouse anti-alpha-tubulin antibodies (Sigma T9026) in 3% BSA, followed by 3 washes with 3% BSA, and then incubated at 37°C for 1 hour in 3% BSA with secondary antibodies (see list in Table S1) followed by 3 washes in PBS. The samples were then post-fixed using 4% Formaldehyde (Sigma 8.18708) during 5 minutes, rinsed 3 times in PBS, quenched in NH4Cl 50 mM for 5 minutes and finally washed 3 times in PBS.

The samples were then mounted on a microscope slide with a drop of Slowfade Diamond ($\approx 8\mu l$) and sealed with twinsil (Picodent). After imaging, the slide was kept in the fridge in the dark.

Data processing

Raw STORM image stacks were processed using using a FIJI macro that runs an analysis with Detection of Molecules (DoM) [28] and Thunderstorm [29], including drift-correction and grouping of consecutive localizations [30]. Further quantification of the blinking quality (Localization precision and number of detections per frame)were performed with UNLOC [31] (see Figures S1-S8). FRC resolution was calculated using a pixel size of 10 nm using the BIOP FIJI plugin [32] with DoM localizations exported in Thunderstorm format to create two images consisting of the odd and even localizations modified from [33,34].

3. Results

3.1. Alexa Fluor 555

We first tested Alexa Fluor 555 (Fig. 1(a)), and observed nice prolonged blinking with individual camera frames showing isolated fluorophores when continuously excited with a 532-nm laser with intensities higher than 1 kW/cm^2 (Fig. 1(b), the raw data is available on zenodo [35]). We imaged the sample continuously to record 20.000 frames , and could reconstruct a high-resolution STORM image (Fig. 1(c-d)). We noticed low photobleaching, and a good number of molecules per frame was still observed after 20,000 frames (See Figure S1). In order to have a quantitative measure of our resolution, we performed a FRC [36] calculation on a 20x20 μm region which yielded a value of 20.5 nm (Fig. 1(e)). Indeed, a profile on the two neighboring microtubules shows that the hollowness of the structure can be resolved (Fig. 1(f)) consistently with the FRC resolution.

3.2. Dye screening

Since Slowfade Diamond is a great buffer for Alexa Fluor 555, we were excited about its potential for multicolor imaging. We first tested a wide array of far-red dyes, as they are the most widely used in STORM, but achieved very poor results with both 640 nm excited dyes such as Alexa Fluor 647 and 750 nm excited dyes such as CF 750. Indeed, they all behaved so poorly (see Table 1) that it was impossible to generate a recognizable image of the structure of interest with any of them.

Undeterred, we moved on to test dyes excited at 488 nm such as Alexa Fluor 488. All 4 dyes we tested (see Table 1) allowed us to at least reconstruct an image of the structure of interest, with Dylight-488 behaving best in that wavelength range. However, the presence of a non-negligible background (partially due to an un-optimized microscope configuration , but also due to the presence of a background signal made particularly significant by our use of epi-illumination that increases with time in our samples, see raw data [35]) required slightly more advanced data

Biomedical Optics EXPRESS

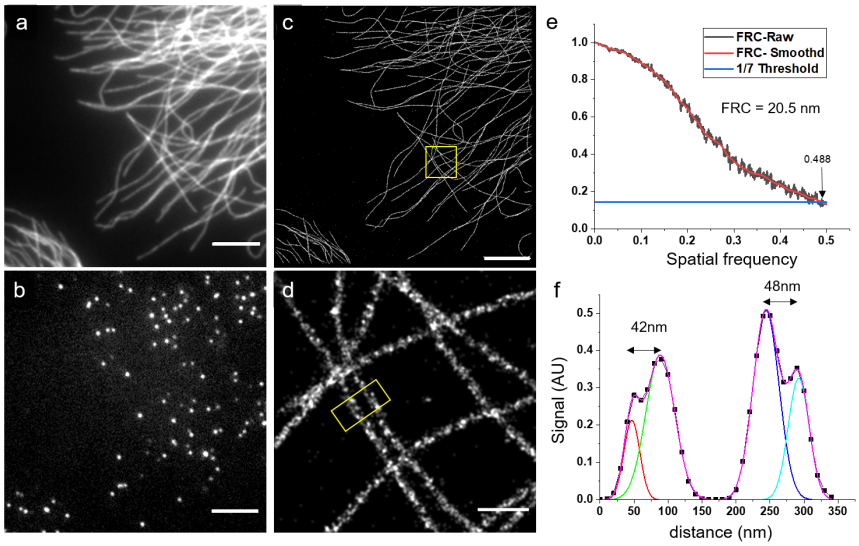

Fig. 1. STORM image of a hCMEC/D3 cell immunostained for alpha-tubulin with Alexa Fluor 555 in Slowfade Diamond. (a) Wide-field image (b) Raw image recorded after a few minutes with continuous high power (>1 kW/cm^2) 532 nm illumination (c) STORM reconstruction of 20,000 raw images, scalebar = 5μm (d) Magnified reconstruction of the inset in (c), scalebar = 500 nm (e) FRC calculation (f) Intensity profile from the region outlined in (d) showing that the hollowness of the microtubules can be resolved. Number of detected molecules in (c): ≈ 1.560 k.

processing: using a temporal median filter [37,38] to remove the slowly varying background we could reconstruct a fairly decent image as can be seen in Fig. 2.

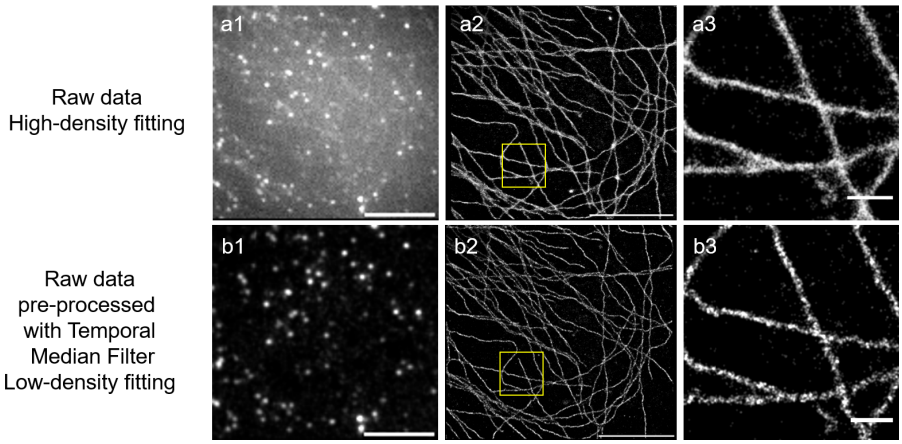

Fig. 2. STORM images of a Cos7 cell immunostained for alpha-tubulin with Dylight-488 in Slowfade Diamond. Due to the high background, we either processed data with a high-density fitting algorithm, (a1-3) or pre-processed the raw data using a temporal median filter (b1-3) Scalebars = 5μm in a1,a2,b1,b2. (a3,b3) magnified view of the regions highlighted in (a2,b2). Scalebars = 500 nm. Number of detected molecules: (a) ≈ 490k (b) ≈ 600k

Biomedical Optics EXPRESS

Table 1. Image quality scale: (-) cannot reconstruct an image. (+) can reconstruct an image at least as good as a widefield image (++) can reconstruct a good quality STORM image [see Figure S2-8 for further quantification] (+++) Best performing dye in Slowfade Diamond. (*) Image quality/FRC after background subtractions

532 nm-excited dyes:

Fluorophore	image quality	FRC (nm)
Alexa Fluor 532	++	29
CF 532	++	28
Alexa Fluor 546	–	-
Dylight 549	++	21
Atto 550	++	25
Alexa Fluor 555	+ + +	20
CF 555	+	-
Cy3	+	-
CF 568	++	20
Alexa Fluor 568	–	-
Alexa Fluor 594	++	24
Dylight 594	++	25

Other dyes:

Fluorophore	image quality	FRC (nm)
Alexa Fluor 488	+	-
CF 488	+	-
Dylight 488	++(*)	35(*)
Alexa Fluor 514	+	-
Alexa Fluor 647	–	-
CF 647	–	-
Dylight 649	–	-
CF 660C	–	-
CF 680	–	-
Alexa Fluor 700	–	-
CF 750	–	-
Dylight 755	–	-

We then considered another option: since Slowfade Diamond works so well for Alexa Fluor 555 maybe it also works with other dyes in that wavelength range that could be used to do multicolor imaging using spectral unmixing [39–41] as is typically done in the usual STORM buffer with Alexa Fluor 647 and CF-680 [20]. We therefore tested 12 different dyes that could be excited at 532 nm, and identified 8 that worked well (see Table 1 and Figure S2-8). Out of these 8 dyes, we chose 3 that have the most distinct emission spectra: Alexa Fluor 532, CF-568 and Alexa Fluor 594 (see Fig. 3(a), spectra taken from FPbase [42]). Images taken with these dyes are shown in Fig. 3(b-d). Although dimmer than Alexa Fluor 555, they all provide high quality STORM images (the raw data is available on zenodo [35]). With the recent advent of publicly available spectral-unmixing software [41,43] we expect this combination to be the most promising for multicolor imaging with Slowfade Diamond.

3.3. Slowfade Diamond as a long-term STORM buffer for Alexa Fluor 555

Since Slowfade Diamond appears to be a suitable buffer for STORM imaging of Alexa Fluor 555, and can be used to preserve mounted samples, we wondered how long samples mounted in Slowfade Diamond could be imaged. We therefore kept a mounted sample in the fridge after imaging, and tried to image it again after 150 and 220 days. As can be seen in Fig. 4, not only could we still image the sample after several months, but the image quality is fairly stable as a function of time. Indeed, performing FRC calculations on the images of the old sample yielded values of 23 nm and 22 nm, compared to 20.5 nm on the fresh sample. We did notice that after 220 days it took longer to reach single molecule regime, and that fairly high laser powers were necessary to obtain a good image, so we expect that $\approx$ 1 year might be a maximum for sample preservation in the fridge. We checked that this was also true after 60 days for the other 532 nm-excited fluorophores rated (++) in Table 1.

Biomedical Optics EXPRESS

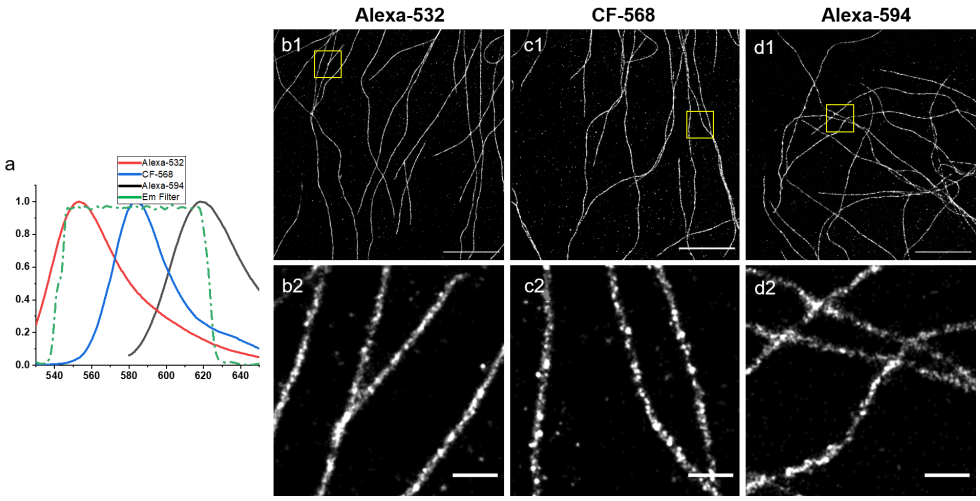

Fig. 3. (a) Emission spectra of Alexa Fluor 532 ,CF 568 and Alexa Fluor 594. (b-d): STORM images of hDBEC cells immunostained for alpha-tubulin with (b) Alexa Fluor 532, (c) CF 568 and (d) Alexa Fluor 594 in Slowfade Diamond. Scalebars = 5μm (b1,c1,d1). (b2,c2,d2): magnified view of the regions highlighted in (a1,b1,c1). Scalebars = 500 nm. Number of detected molecules: (b) ≈ 570k (c) ≈ 450k (d) ≈ 760k.

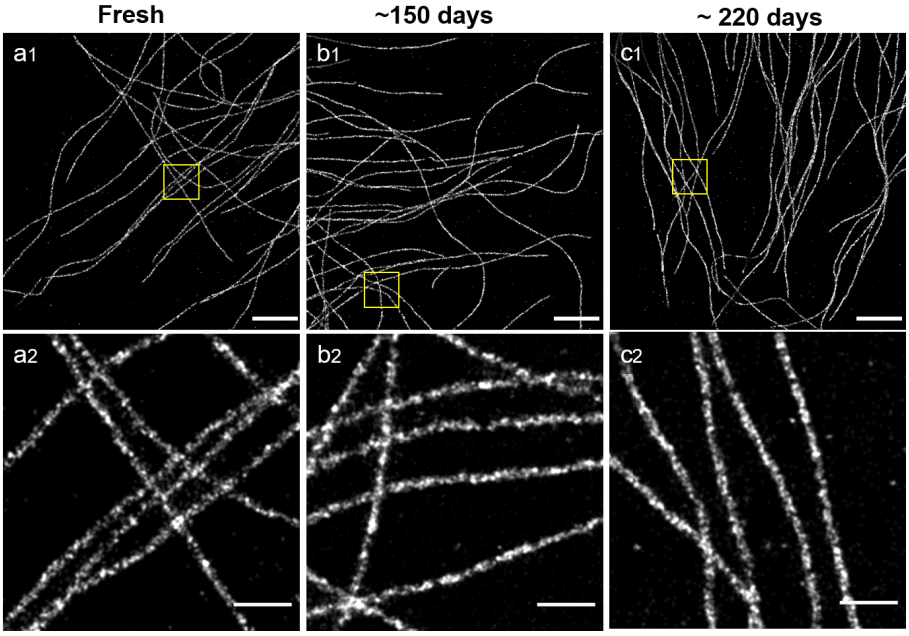

Fig. 4. STORM images of hCMEC/D3 cells immunostained for alpha-tubulin with Fluor 555 in Slowfade Diamond as a function of time after mounting the sample: Sample imaged just after mounting (a1), 150 days after mounting (b1) and 220 days after mounting (c1) Scalebars = 5μm. (a2,b2,c2) magnified view of the regions highlighted in (a1,b1,bc1). Scalebars = 500 nm Number of detected molecules: (a) ≈ 1550k (b) ≈ 3250k (c) ≈ 1450k.

Biomedical Optics EXPRESS

4. Conclusion and perspectives

We tested 24 different fluorophores in Slowfade Diamond and found that a surprisingly large number of 532 nm excited dyes blinked very well, as well as to a lesser degree all the 488 nm excited dyes we tried. Interestingly, samples mounted in Slowfade and kept in the fridges can be imaged for several month which should be very useful for microscope calibration and comparisons, as well as for teaching (The bright signal of the single red fluorophores can be readily observed by eye on the eyepiece). The composition of Slowfade Diamond being proprietary information, it is hard to draw conclusion about the photophysics involved [17,18], but it is interesting to notice the high correlation between dyes that work and the excitation wavelength used, and the fact that the wavelength range that works well is very different to that of the usual buffer [19,20] or of Vectashield [21]. The index of refraction of Slowfade Diamond is 1.42, so TIRF and grazing incidence imaging are both possible (though they require the use of high NA objective), as well as the use of an active z-stabilization but the higher index compared to that of most water-based buffer limits depth-induced aberrations, which is especially relevant for 3D imaging. As was the case with Vectashield, one potential advantage of using a common mounting medium as Slowfade Diamond would be to combine SIM [44,45] and STORM for multicolor imaging, for example with 405-nm and 488-nm excited fluorophores used for SIM and one or two 532 nm excited dye used for STORM. Slowfade Diamond has also been used for STED microscopy [46,47] (see Figure S9) but since it is a scanning technique, straightforward combinations seem difficult. However, comparisons could be performed on the same sample between SIM, STED and STORM, for example for metrology or to determine which method is better adapted to a particular sample. Finally, since Vectashield works for far-red fluorophores, an intriguing possibility would be to mix the two anti-fading agents to achieve multi-color imaging.

Funding. Institut de physique (Tremplin@INP 2019, Tremplin@INP 2021).

Acknowledgments. We thank Sandrine Lévêque-Fort for the Cos-7 cells, Maxime Mauviel for his help with Cos-7 cell culture, and Mathieu Coureuil for his help with hCMEC/D3 cell culture. We also thank Vectorlab for the gift of the Dylight-488, Dylight-549, Dylight-594 and Dylight-649 antibodies, Biotium for the gift of the CF 532, CF 660C, and CF 680 secondary antibodies. We thank Debora Keller-Olivier for critical reading, and all the members of the "nano" group at LOB for scientific and technical discussions. N.O. thanks Christa Walther and the imaging facility at the University of Sheffield for preliminary experiments.

Disclosures. The authors declare no conflicts of interest

Data availability. Data underlying the results presented in this paper are available on Zenodo [35].

Supplemental document. See Supplement 1 for supporting content.

References

1. M. J. Rust, M. Bates, and X. Zhuang, "Sub-diffraction-limit imaging by stochastic optical reconstruction microscopy (storm)," Nat. Methods **3**(10), 793–796 (2006).
2. E. Betzig, G. H. Patterson, R. Sougrat, O. W. Lindwasser, S. Olenych, J. S. Bonifacino, M. W. Davidson, J. Lippincott-Schwartz, and H. F. Hess, "Imaging intracellular fluorescent proteins at nanometer resolution," Science **313**(5793), 1642–1645 (2006).
3. S. T. Hess, T. P. Girirajan, and M. D. Mason, "Ultra-high resolution imaging by fluorescence photoactivation localization microscopy," Biophys. J. **91**(11), 4258–4272 (2006).
4. A. Sharonov and R. M. Hochstrasser, "Wide-field subdiffraction imaging by accumulated binding of diffusing probes," Proc. Natl. Acad. Sci. **103**(50), 18911–18916 (2006).
5. R. Jungmann, C. Steinhauer, M. Scheible, A. Kuzyk, P. Tinnefeld, and F. C. Simmel, "Single-molecule kinetics and super-resolution microscopy by fluorescence imaging of transient binding on dna origami," Nano Lett. **10**(11), 4756–4761 (2010).
6. M. Lelek, M. T. Gyparaki, G. Beliu, F. Schueder, J. Griffié, S. Manley, R. Jungmann, M. Sauer, M. Lakadamyali, and C. Zimmer, "Single-molecule localization microscopy," Nat. Rev. Methods Primers **1**(1), 39 (2021).
7. M. Bates, T. R. Blosser, and X. Zhuang, "Short-range spectroscopic ruler based on a single-molecule optical switch," Phys. Rev. Lett. **94**(10), 108101 (2005).
8. M. Heilemann, E. Margeat, R. Kasper, M. Sauer, and P. Tinnefeld, "Carbocyanine dyes as efficient reversible single-molecule optical switch," J. Am. Chem. Soc. **127**(11), 3801–3806 (2005).

Biomedical Optics EXPRESS

9. C. Steinhauer, C. Forthmann, J. Vogelsang, and P. Tinnefeld, "Superresolution microscopy on the basis of engineered dark states," J. Am. Chem. Soc. **130**(50), 16840–16841 (2008).
10. R. E. Benesch and R. Benesch, "Enzymatic removal of oxygen for polarography and related methods," Science **118**(3068), 447–448 (1953).
11. X. Shi, J. Lim, and T. Ha, "Acidification of the oxygen scavenging system in single-molecule fluorescence studies: in situ sensing with a ratiometric dual-emission probe," Anal. Chem. **82**(14), 6132–6138 (2010).
12. T. M. Hartwich, K. K. H. Chung, L. Schroeder, J. Bewersdorf, C. Soeller, and D. Baddeley, "A stable, high refractive index, switching buffer for super-resolution imaging," bioRxiv, 465492 (2018).
13. C. E. Aitken, R. A. Marshall, and J. D. Puglisi, "An oxygen scavenging system for improvement of dye stability in single-molecule fluorescence experiments," Biophys. J. **94**(5), 1826–1835 (2008).
14. N. Olivier, D. Keller, P. Gönczy, and S. Manley, "Resolution doubling in 3D-storm imaging through improved buffers," PLoS One **8**(7), e69004 (2013).
15. M. Swoboda, J. Henig, H.-M. Cheng, D. Brugger, D. Haltrich, N. Plumeré, and M. Schlierf, "Enzymatic oxygen scavenging for photostability without pH drop in single-molecule experiments," ACS Nano **6**(7), 6364–6369 (2012).
16. G. T. Dempsey, M. Bates, W. E. Kowtoniuk, D. R. Liu, R. Y. Tsien, and X. Zhuang, "Photoswitching mechanism of cyanine dyes," J. Am. Chem. Soc. **131**(51), 18192–18193 (2009).
17. M. Levitus, "Photophysics of single-molecule probes," in *Spectroscopy and Dynamics of Single Molecules*, (Elsevier, 2019), pp. 15–69.
18. T. Ha and P. Tinnefeld, "Photophysics of fluorescent probes for single-molecule biophysics and super-resolution imaging," Annu. Rev. Phys. Chem. **63**(1), 595–617 (2012).
19. G. T. Dempsey, J. C. Vaughan, K. H. Chen, M. Bates, and X. Zhuang, "Evaluation of fluorophores for optimal performance in localization-based super-resolution imaging," Nat. Methods **8**(12), 1027–1036 (2011).
20. M. Lehmann, G. Lichtner, H. Klenz, and J. Schmoranzer, "Novel organic dyes for multicolor localization-based super-resolution microscopy," J. Biophotonics **9**(1-2), 161–170 (2016).
21. N. Olivier, D. Keller, V. S. Rajan, P. Gönczy, and S. Manley, "Simple buffers for 3D storm microscopy," Biomed. Opt. Express **4**(6), 885–899 (2013).
22. K. Kwakwa, A. Savell, T. Davies, I. Munro, S. Parrinello, M. A. Purbhoo, C. Dunsby, M. A. Neil, and P. M. French, "Easystorm: a robust, lower-cost approach to localisation and tirf microscopy," J. Biophotonics **9**(9), 948–957 (2016).
23. A. Arsić, N. Stajković, R. Spiegel, and I. Nikić-Spiegel, "Effect of vectashield-induced fluorescence quenching on conventional and super-resolution microscopy," Sci. Rep. **10**(1), 6441 (2020).
24. K. Prakash, "Laser-free super-resolution microscopy," Phil. Trans. R. Soc. A **379**(2199), 20200144 (2021).
25. A. D. Edelstein, M. A. Tsuchida, N. Amodaj, H. Pinkard, R. D. Vale, and N. Stuurman, "Advanced methods of microscope control using μmanager software," J. Biol. Methods **1**(2), e10 (2014).
26. B. Weksler, E. Subileau, N. Perriere, P. Charneau, K. Holloway, M. Leveque, H. Tricoire-Leignel, A. Nicotra, S. Bourdoulous, P. Turowski, D. K. Male, F. Roux, J. Greenwood, I. A. Romero, and P. O. Couraud, "Blood-brain barrier-specific properties of a human adult brain endothelial cell line," FASEB J. **19**(13), 1872–1874 (2005).
27. J.-P. Barnier, J. Meyer, S. Kolappan, H. Bouzinba-Ségard, G. Gesbert, A. Jamet, E. Frapy, S. Schönherr-Hellec, E. Capel, Z. Virion, M. Dupuis, E. Bille, P. Morand, T. Schmitt, S. Bourdoulous, X. Nassif, L. Craig, and M. Coureuil, "The minor pilin pilv provides a conserved adhesion site throughout the antigenically variable meningococcal type iv pilus," Proc. Natl. Acad. Sci. **118**(45), e2109364118 (2021).
28. A. Chazeau, E. A. Katrukha, C. C. Hoogenraad, and L. C. Kapitein, "Studying neuronal microtubule organization and microtubule-associated proteins using single molecule localization microscopy," in *Methods in Cell Biology*, vol. 131 (Elsevier, 2016), pp. 127–149.
29. K. J. Martens, A. N. Bader, S. Baas, B. Rieger, and J. Hohlbein, "Phasor based single-molecule localization microscopy in 3d (PSMLM-3d): An algorithm for mhz localization rates using standard cpus," J. Chem. Phys. **148**(12), 123311 (2018).
30. "Fiji macros for storm analysis," GitHub, https://github.com/LaboratoryOpticsBiosciences/STORM_Analysis.
31. S. Mailfert, J. Touvier, L. Benyoussef, R. Fabre, A. Rabaoui, M.-C. Blache, Y. Hamon, S. Brustlein, S. Monneret, D. Marguet, and N. Bertaux, "A theoretical high-density nanoscopy study leads to the design of unloc, a parameter-free algorithm," Biophys. J. **115**(3), 565–576 (2018).
32. B. (EPFL), "Biop FRC imagej macro," GitHub, 2022, https://github.com/BIOP/ijp-frc.
33. C. Letterier, "Christorm fiji macros," GitHub, 2022, https://github.com/cleterrier/ChriSTORM.
34. C. Leterrier, J. Potier, G. Caillol, C. Debarnot, F. R. Boroni, and B. Dargent, "Nanoscale architecture of the axon initial segment reveals an organized and robust scaffold," Cell Rep. **13**(12), 2781–2793 (2015).
35. H. Boukhatem, B Durel, and M. Raimbault, *et al.*, "Raw storm data," Zenodo 2022, https://doi.org/10.5281/zenodo.7054330.
36. R. P. Nieuwenhuizen, K. A. Lidke, M. Bates, D. L. Puig, D. Grünwald, S. Stallinga, and B. Rieger, "Measuring image resolution in optical nanoscopy," Nat. Methods **10**(6), 557–562 (2013).
37. E. Hoogendoorn, K. C. Crosby, D. Leyton-Puig, R. M. Breedijk, K. Jalink, T. W. Gadella, and M. Postma, "The fidelity of stochastic single-molecule super-resolution reconstructions critically depends upon robust background estimation," Sci. Rep. **4**(1), 3854 (2015).
38. H. Lab, "Fast temporal median filter fiji plugin," Github, 2022, https://github.com/HohlbeinLab/FTM2.

Biomedical Optics EXPRESS

39. E. Platonova, C. M. Winterflood, and H. Ewers, "A simple method for gfp-and rfp-based dual color single-molecule localization microscopy," ACS Chem. Biol. **10**(6), 1411–1416 (2015).
40. C. M. Winterflood, E. Platonova, D. Albrecht, and H. Ewers, "Dual-color 3d superresolution microscopy by combined spectral-demixing and biplane imaging," Biophys. J. **109**(1), 3–6 (2015).
41. L. Andronov, R. Genthial, D. Hentsch, and B. P. Klaholz, "A spectral demixing method for high-precision multi-color localization microscopy," bioRxiv, bioRxiv:2021.12.23.473862 (2021).
42. T. J. Lambert, "Fpbase: a community-editable fluorescent protein database," Nat. Methods **16**(4), 277–278 (2019).
43. J. Ries, "Smap: a modular super-resolution microscopy analysis platform for smlm data," Nat. Methods **17**(9), 870–872 (2020).
44. M. G. Gustafsson, "Surpassing the lateral resolution limit by a factor of two using structured illumination microscopy," J. Microsc. **198**(2), 82–87 (2000).
45. L. Schermelleh, P. M. Carlton, S. Haase, L. Shao, L. Winoto, P. Kner, B. Burke, M. C. Cardoso, D. A. Agard, M. G. Gustafsson, H. Leonhardt, and J. W. Sedat, "Subdiffraction multicolor imaging of the nuclear periphery with 3d structured illumination microscopy," Science **320**(5881), 1332–1336 (2008).
46. S. W. Hell and J. Wichmann, "Breaking the diffraction resolution limit by stimulated emission: stimulated-emission-depletion fluorescence microscopy," Opt. Lett. **19**(11), 780–782 (1994).
47. F. Görlitz, S. Guldbrand, T. H. Runcorn, R. T. Murray, A. L. Jaso-Tamame, H. G. Sinclair, E. Martinez-Perez, J. R. Taylor, M. A. Neil, C. Dunsby, and P. M. French, "Easyslm-sted: Stimulated emission depletion microscopy with aberration correction, extended field of view and multiple beam scanning," J. Biophotonics **11**(11), e201800087 (2018).